Journal of Molecular Structure 1100 (2015) 80–87

Contents lists available at ScienceDirect

Journal of Molecular Structure

journal homepage: http://www.elsevier.com/locate/molstruc

Gas phase reaction of phosphorus trichloride and methanol: Matrix isolation infrared and *DFT* studies

Prasad Ramesh Joshi, N. Ramanathan, K. Sundararajan, K. Sankaran*

Materials Chemistry Division, Chemistry Group, Indira Gandhi Center for Atomic Research, Kalpakkam 603102, Tamil Nadu, India

ARTICLE INFO

Article history:
Received 5 June 2015
Received in revised form
15 July 2015
Accepted 15 July 2015
Available online 17 July 2015

Keywords:
Phosphorus trichloride
Methanol: gas phase reaction
Matrix isolation infrared spectroscopy
DFT calculation

ABSTRACT

Gas phase reaction of phosphorus trichloride (PCl_3) and methanol (CH_3OH) was carried out with different ratios of PCl_3:CH_3OH:N_2 (1:1:1000, 1:2:1000 and 1:3:1000) and the products were identified using matrix isolation infrared spectroscopy. For the 1:1 and 1:2 ratios of PCl_3:CH_3OH, dichloro methyl phosphite (DCMP) and methyl chloride (CH_3Cl) were the products formed. Interestingly, only methyl chloride (CH_3Cl) was observed for the 1:3 ratio of PCl_3:CH_3OH. DFT computations were carried out at B3LYP/6-311++G(d,p) level of theory to give insights into the formation of the reaction products. Based on the experimental findings and computations a reaction mechanism has been proposed through a *nucleophilic* substitution reaction to explain the formation of the products.

1. Introduction

Organophosphorus chemistry is an interdisciplinary subject which deals with the study of organic carbon and inorganic phosphorus moity. The interest on the study of this discipline is growing rapidly owing to the application of organophosphorus compounds in various fields such as pesticide, drug, polymer, perfume, paint stripper, protective coating and automobile industries [1–3]. The rapid development of the above subject to date also helped to understand the biochemistry involving organophosphorus compounds such as the synthesis of DNA that operates through phosphite intermediate followed by its oxidation to phosphate, a stable form of organophosphorous compound, during the synthesis. The study of phosphites (phosphorus esters) and their reactions are particularly important as these serve as model systems for understanding many biological reactions [4–7].

One of the simplest ways for the synthesis of phosphonates and phosphites is the reaction between phosphorus trichloride (PCl_3) and alcohol. Trimethyl phosphite (TMPhite) is synthesized in a controlled manner when 3 mol of methanol is mixed with 1 mol of PCl_3 in an inert solvent like hexane or heptane at low temperatures [8]. TMPhite is an industrially important compound as it is used for the synthesis of phosphorus doped diamond films in electronic industries [9]. It is also used for improving the performance of electrolytic systems [10].

Since, the reaction involving PCl_3 precursor found applications at various stages of synthesis, it is important to understand the mechanism and progress of the reaction as a function of stoichiometry. By and large, organic synthesis is performed in the condensed phase in presence of a solvent. In a solvent medium, the transportation of reactants is aided by the solvent molecules in contrast to gas phase reaction. However, the effect of solvent can lead to an ambiguous interpretation while understanding the mechanism of the reaction [11]. For instance, it is necessary to take into account the solvation energies of intermediates participating in the reaction as ascribed due to solvation by solvent molecules [12]. On the contrary, gas phase studies provide an ideal milieu for understanding elementary chemical reactions without any perturbation from the surrounding solvent molecules. Further, gas phase reactions are found to be beneficial as it can directly be corroborated with computational studies. Laerdahl and Uggerud have reviewed the gas phase nucleophilic reactions with theoretical data [13]. Mass spectroscopy was used as a characterization technique while studying those reactions.

Owing to the superior resolution that can be obtained in a matrix isolation experiment, this technique in combination with infrared spectroscopy can be best explored for studying the gas phase reactions. Recently, using matrix isolation infrared spectroscopy, the gas phase nucleophilic reaction of trimethyl phosphite (TMPhite) with HCl was probed. When the precursors were premixed prior to deposition in a N_2 matrix at 12 K, methyl chloride

* Corresponding author.
E-mail address: ksran@igcar.gov.in (K. Sankaran).

http://dx.doi.org/10.1016/j.molstruc.2015.07.028
0022-2860/

was observed as the product. The reaction followed Arbuzov pathway and proceeded through the lone pair on the phosphorus as a nucleophilic centre [14]. In another study, gas phase nucleophilic reaction between dimethoxy methane (DMM) and HCl was reported with HCl as a nucleophile. Though DMM possesses both methylenic and methyl carbon atoms, only methylenic pathway was preferred in the gas phase producing chloromethyl methyl ether (CMME) and methanol [15].

In the present study, matrix isolation infrared technique was used to trap and identify the product formed in the gas phase reaction between PCl_3 and CH_3OH. DFT computations were carried out to support our experimental results.

2. Experimental and computational methods

The prerequisite of a low temperature for matrix isolation experiments was achieved using a RDX-408D2 (Sumitomo Heavy Industries Ltd.) pulsed tube, closed cycle helium compressor cooled cryostat. A base pressure of less than 1×10^{-6} mbar was obtained in the cryostat housed to an evacuated vacuum chamber.

Analytical grade PCl_3 (Merck, Purity: > 99%) and HPLC grade CH_3OH (Purity: >99%) were used without any further purification. However, the samples were subjected to several freeze-pump-thaw cycles before its use. Nitrogen (INOX) with a purity of 99.9995% was used as the matrix gas. PCl_3 and CH_3OH were premixed in a glass bulb having 1 dm^3 volume along with nitrogen, as a matrix gas, at room temperature. Three experiments were performed by varying the concentration of CH_3OH and keeping PCl_3 concentration constant such as a) PCl_3:CH_3OH:N_2 (1:1:1000), b) PCl_3:CH_3OH:N_2 (1:2:1000) and c) PCl_3:CH_3OH:N_2 (1:3:1000) to understand the effect of stoichiometry. A typical deposition lasted for about 90 min at ~3 mmol/h rate.

Infrared spectra of the matrix-isolated samples were recorded in transmission mode between 4000 and 400 cm^{-1} using a BOMEM MB 100 FTIR spectrometer with 1 cm^{-1} resolution. All the spectra reported here are those obtained after deposition of samples onto a KBr substrate maintained at 12 K.

Computations were performed using a Gaussian 94W package [16] at B3LYP/6-311++G(d,p) level of theory without imposing any geometrical constraints. Geometries of reactants (PCl_3 and CH_3OH) and possible products were optimized by keeping all geometrical parameters free during optimization process. The optimized geometries were then used to obtain vibrational frequencies which enable us to characterize the nature of stationary points and to assign the experimentally obtained frequencies. The computed vibrational frequencies were scaled on a mode-by-mode basis for the different modes for assigning the experimental features. It is recognized that matrix perturbs vibrational frequencies of the trapped species, with the magnitude of perturbation depending upon vibrational frequency of the mode. We therefore consider that a mode-by-mode scaling is an appropriate method to account for the varying degrees of matrix influence and helps in bringing the computations in better agreement with experimental values over the entire range of the vibrational wavenumbers [17–22]. The conformational isomers of the reaction products were also studied. The computed intensities and scaled frequencies were used before plotting a simulated vibrational spectrum using SYNSPEC program [23] where a Lorentzian line profile with a full-width-at-half-maximum of 1 cm^{-1} was assumed.

3. Results and discussion

3.1. Experimental section

Three experiments with different ratios of PCl_3:CH_3OH such as 1:1, 1:2 and 1:3 in gas phase were studied by varying the concentration of CH_3OH to understand the reaction progress against stoichiometry. For clarity, IR spectra are discussed in four regions (520–450 cm^{-1}, 760–720 cm^{-1}, 1050–1020 cm^{-1}, and 3050–2920 cm^{-1}).

Fig. 1 (grid A) shows infrared spectra corresponding to the P–Cl stretching vibrational mode in a N_2 matrix. The doubly degenerate P–Cl stretching mode [ν_3(e)] of PCl_3 has been reported to occur at 498.9 and 494.9 cm^{-1} and the non-degenerate P–Cl stretching mode [$\nu_1(a_1)$] at 510.4 and 508.8 cm^{-1} in an Ar Matrix [24]. The ν_3(e) mode of PCl_3 is observed at 496.6 and 492.3 cm^{-1} and the $\nu_1(a_1)$ mode at 511.1 and 509.2 cm^{-1} in a N_2 matrix (Fig. 1a, grid A). Multiple features observed in the ν_3(e) mode in N_2 matrix has already been assigned to i) isotopic effect of chlorine (^{35}Cl:^{37}Cl = 3:0/2:1/1:2), ii) splitting of degenerate vibrational states due to the host matrix atoms and iii) matrix site effect or unification of two or more of these effects [25].

When PCl_3 and CH_3OH were premixed in a 1:1 ratio along with N_2 gas in a bulb and the resultant gas mixture was deposited on to a cryotip at 12 K, infrared spectra showed new features at 469.2, 466.4, 464.5, 462.1 cm^{-1} and a broad feature at 511.3 cm^{-1} apart from the parent P–Cl stretching features of PCl_3 (Fig. 1c). Importantly, intensities of P–Cl features of the parent PCl_3 did drop down at the expense of new features. When experiments were carried out with 1:2 PCl_3:CH_3OH ratio, we observed the same new features as in the case of 1:1 PCl_3:CH_3OH but the parent PCl_3 peaks were completely disappeared. The infrared intensities of the product features were relatively high when compared to the 1:1 PCl_3:CH_3OH experiment (Fig. 1d, grid A). Interestingly, none of the above new features were observed in the P–Cl stretching region, when 1:3 PCl_3:CH_3OH experiment was performed (Fig. 1e, grid A).

In the 760–720 cm^{-1} region, for 1:1 ratio of PCl_3 and CH_3OH along with N_2 gas (Fig. 1c, grid B), a strong feature at 753.1 cm^{-1} and weak features at 732.5 and 726.9 cm^{-1} were observed. In the case of 1:2 PCl_3:CH_3OH experiment (Fig. 1d, grid B), alike 1:1 PCl_3:CH_3OH experiment, all three features were observed. The intensity of the features at 732.5 and 726.9 cm^{-1} were higher and no significant change in the intensity of 753.1 cm^{-1} feature was observed. In the case of 1:3 PCl_3:CH_3OH experiment (Fig. 1e, grid B), the 753.1 cm^{-1} feature was completely absent, while the features at 732.5 and 726.9 cm^{-1} were observed with highest intensity.

In the 1050–1020 cm^{-1} region, Fig. 1b (grid C) the feature observed at 1034.0 cm^{-1} corresponds to O–C stretch of monomeric CH_3OH [26–28]. When 1:1 PCl_3:CH_3OH experiment (Fig. 1c, grid C) in N_2 matrix was performed, the feature due to O–C stretching of CH_3OH was absent and new strong features at 1044.4 and 1042.1 cm^{-1} and a weak feature at 1026.8 cm^{-1} were observed. Similar observation was noticed, in the 1:2 PCl_3:CH_3OH experiment (Fig. 1d, grid C) but the intensity of the feature at 1026.8 cm^{-1} was found to be increased. No parent signature of O–C stretch at 1034.0 cm^{-1} was seen in this experiment, confirming the complete reaction of CH_3OH with PCl_3. In the case of 1:3 PCl_3:CH_3OH experiment (Fig. 1e, grid C), apart from the feature due to O–C stretch of monomeric CH_3OH, the 1026.8 cm^{-1} feature was observed with increased intensity.

In the 3000–2800 cm^{-1} region, a new feature at 2853.7 cm^{-1} along with a low intense feature at 2963.3 cm^{-1} were observed in 1:1 PCl_3:CH_3OH experiment (Fig. 1c, grid D) which did grow substantially in the 1:2 PCl_3:CH_3OH experiment (Fig. 1d, grid D). Whereas for the 1:3 PCl_3:CH_3OH (Fig. 1e, grid D) experiment, the intensity of the feature at 2853.7 cm^{-1} decreased considerably and the intensity of the 2963.3 cm^{-1} feature increased.

New features observed in all the aforementioned spectra in the different regions indicate that the reactants PCl_3 and CH_3OH undergo reaction to yield new products. Importantly, these new

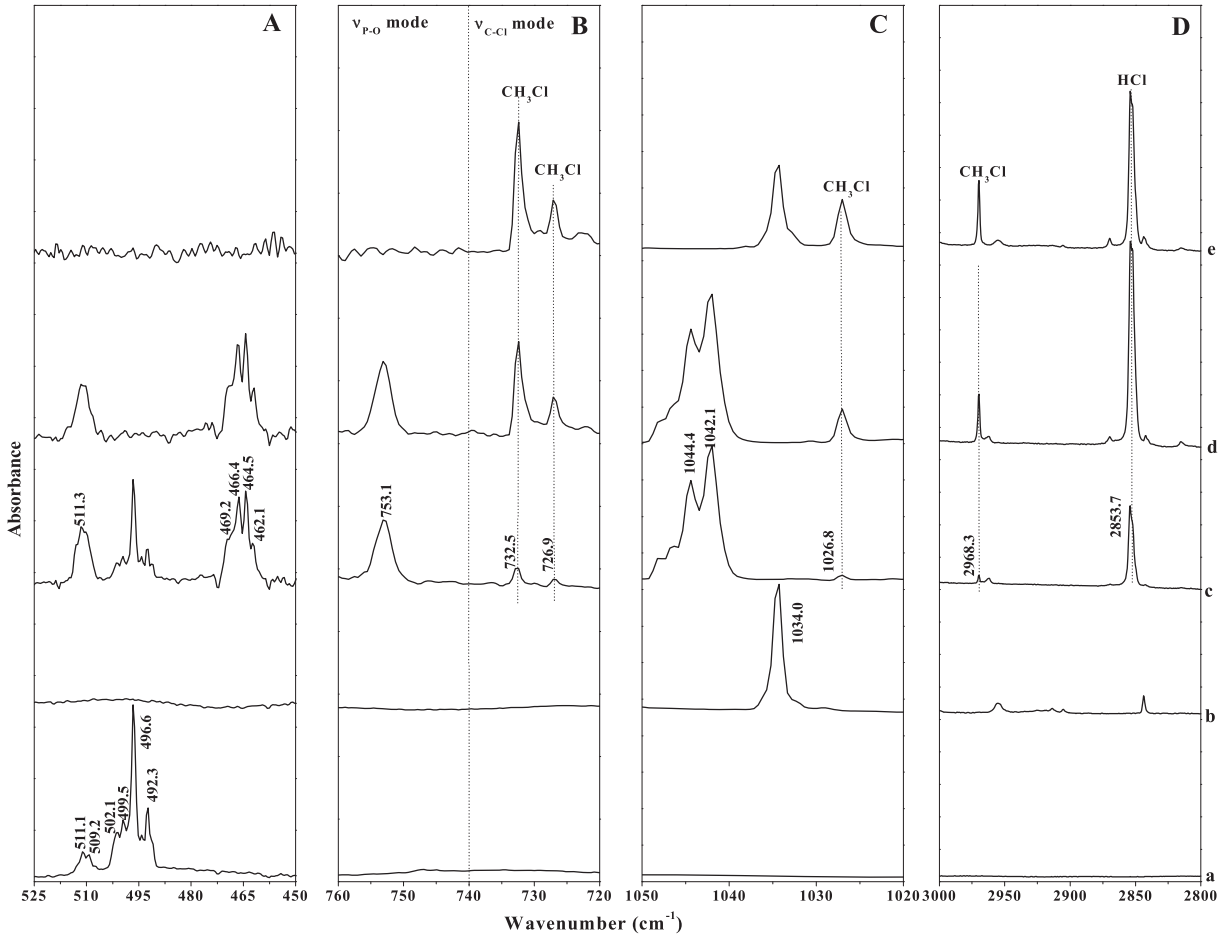

Fig. 1. Matrix isolation infrared spectra in a N_2 matrix in the region 525–450 cm^{-1} (Grid A); 760–720 cm^{-1} (Grid B); 1050–1020 cm^{-1} (Grid C) and 3000–2800 cm^{-1} (Grid D): a) PCl_3:N_2 (1:1000); b) CH_3OH:N_2 (1:1000); c) PCl_3:CH_3OH:N_2 (1:1:1000); d) PCl_3:CH_3OH:N_2 (1:2:1000); e) PCl_3:CH_3OH:N_2 (1:3:1000).

features are not due to the PCl_3–CH_3OH adducts in the N_2 matrix, as the adduct features were characterized in the earlier study [25].

Nucleophilic reaction could be the probable avenue for the products formed during PCl_3 and CH_3OH reaction. Both CH_3OH and PCl_3 can act as nucleophile due to the presence of lone pairs of electrons on the oxygen and chlorine atoms respectively. The possibility of PCl_3 as a nucleophile due to phosphorus lone pair is ruled out (a case of Arbuzov reaction) due to the presence of three electron withdrawing chlorine atoms which pulls electron cloud away from phosphorus atom making the phosphorus more electrophilic in nature. Therefore, the envisaged product formed in the 1:1 PCl_3:CH_3OH experiment is either dichloromethylphosphite (DCMP) and HCl (formed due to the nucleophilic oxygen) or dichlorohydroxyphosphite (DCHP) and CH_3Cl (formed due to PCl_3 by virtue of nucleophilic chlorine atom) as per the following reactions.

$$PCl_3 + CH_3OH \rightarrow CH_3OPCl_2 + HCl \quad (1)$$

$$PCl_3 + CH_3OH \rightarrow HOPCl_2 + CH_3Cl \quad (2)$$

A closer examination of the infrared features of the products revealed that one of the products of the PCl_3:CH_3OH reaction is HCl, as the feature at 2853.7 cm^{-1} is characteristic of HCl in a N_2 matrix [14]. This indicates that the other product could be DCMP produced through the reaction (1). Based on this, the new features at 1044.4, 1042.1, 753.1, 511.3, 469.2, 466.4, 464.5 and 462.1 cm^{-1} could be tentatively assigned to DCMP. For the 1:2 and 1:3 PCl_3:CH_3OH experiments one can expect successive replacement of Cl atoms of PCl_3 by methoxy ($-OCH_3$) groups to form dimethylchloro phosphite (DMCP) and trimethyl phosphite (TMPhite) as shown in the following reactions:

$$PCl_3 + 2\ CH_3OH \rightarrow (CH_3O)_2PCl + 2\ HCl \quad (3)$$

$$PCl_3 + 3\ CH_3OH \rightarrow (CH_3O)_3P + 3\ HCl \quad (4)$$

The infrared features observed in the case of 1:2 PCl_3:CH_3OH experiment are similar to that of 1:1 PCl_3:CH_3OH experiment. However, the product expected based on the reaction (3) is DMCP which we expect to have different IR features from that of DCMP produced in the 1:1 PCl_3:CH_3OH experiment. A detailed discussion on this topic is given in the forthcoming section.

Interestingly, in the case of 1:3 PCl_3:CH_3OH experiment, strong features were observed at 732.6 and 727.3 cm^{-1} (Fig. 1e, grid B), 1026.8 (Fig. 1e, grid C), 2968.3 (Fig. 1e grid D), and 3048.2, 2870.2, 1445.4 and 1353.4 cm^{-1} (not shown in Fig.) in N_2 matrix. These intense product bands listed above agree well with the features reported for CH_3Cl in a N_2 matrix [14]. It is important to point out that small amount of CH_3Cl was produced even in the 1:1 PCl_3:CH_3OH experiment, but the amount of which progressively increased in 1:2 and 1:3 PCl_3:CH_3OH experiments.

3.1.1. *Mechanism predicted on the basis of experimental results*

From the above observations, it can be reckoned that alike any normal second-order nucleophilic substitution (S_N2) reaction, the

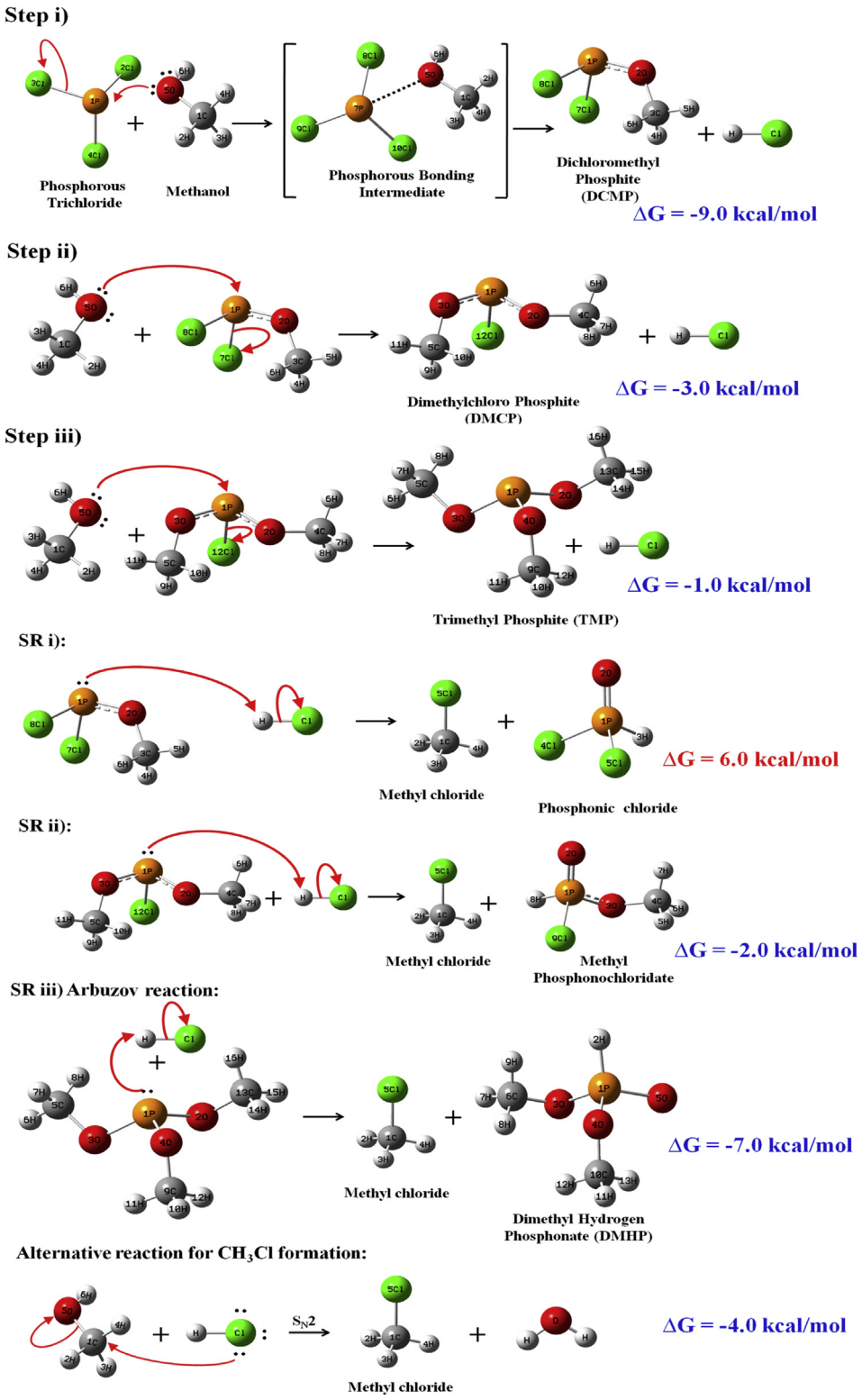

Fig. 2. Schematic representation of reaction mechanism predicted for PCl_3 and CH_3OH reaction. ΔG represents the free energy change of reaction computed at B3LYP/6-311++G(d,p) level of theory. * SR = side reaction.

reaction between PCl_3 and CH_3OH may proceed to form the product, DCMP in the case of 1:1 PCl_3:CH_3OH stochiometric experiment. In this reaction, CH_3OH acts as a nucleophile. The lone pair of electrons on oxygen of CH_3OH attacks the electrophilic phosphorus of PCl_3 with a simultaneous cleavage of one of the P—Cl bonds and the product DCMP is formed as shown in Fig. 2 (step i) through an intermediate. Experimental evidence for the *phosphorus bonding* intermediate has been recently reported, when PCl_3 and CH_3OH were co-deposited through twin-jet nozzle in a N_2 matrix instead of premixing the gases and then deposited [25]. Recently, extensive

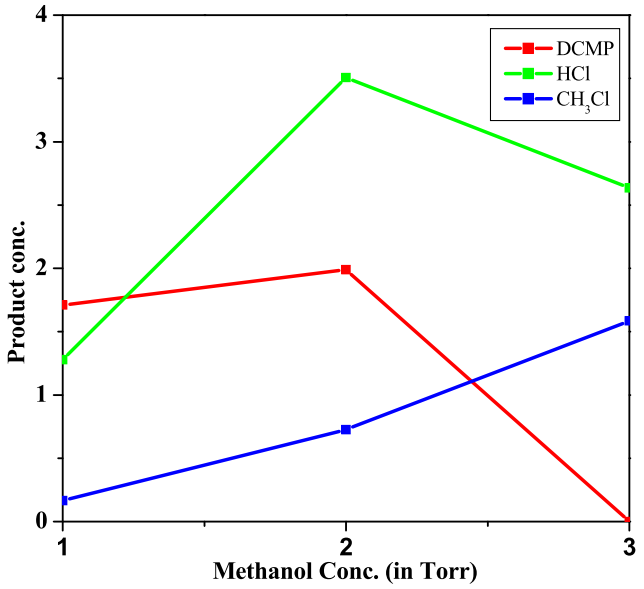

Fig. 3. A plot of product concentrations against CH_3OH concentration.

computational studies on this kind of intermolecular interaction were reported by Schiener et al. [29–38] and Del Bene et al. [39–43] and named it as pnictogen bonding or more specifically *phosphorus bonding*. The phosphorus bonded adduct can be considered to be the initial intermediate for the reaction between PCl_3 and CH_3OH in the gas phase Fig. 2 (Step i). We believe that for all the ratios of PCl_3 and CH_3OH the reaction proceeds via step (i) but the concentration of methanol plays a crucial role in the formation of the different products. Fig. 3 shows the plot of area of products formed during reaction against methanol concentration for various ratios of PCl_3:CH_3OH.

As pointed out earlier, we do observe IR features due to CH_3Cl in the 1:1 PCl_3:CH_3OH experiment (Fig 1c). Two possible pathways could be thought of for the formation of CH_3Cl: (a) a reaction between DCMP and HCl (Fig. 2, SR i) and (b) reaction between the HCl obtained in step (i) with CH_3OH. A separate experiment on premixing of CH_3OH and HCl confirmed the formation of CH_3Cl. Fig. 1c (grid A) shows the presence of infrared features of unreacted PCl_3 in the 1:1 PCl_3:CH_3OH experiment indicating that some of the CH_3OH could have been used for reacting with HCl.

In case of 1:2 PCl_3:CH_3OH experiment, no infrared features of PCl_3 was observed indicating that all the PCl_3 were consumed in the reaction. The DCMP formed in the first step could have reacted with

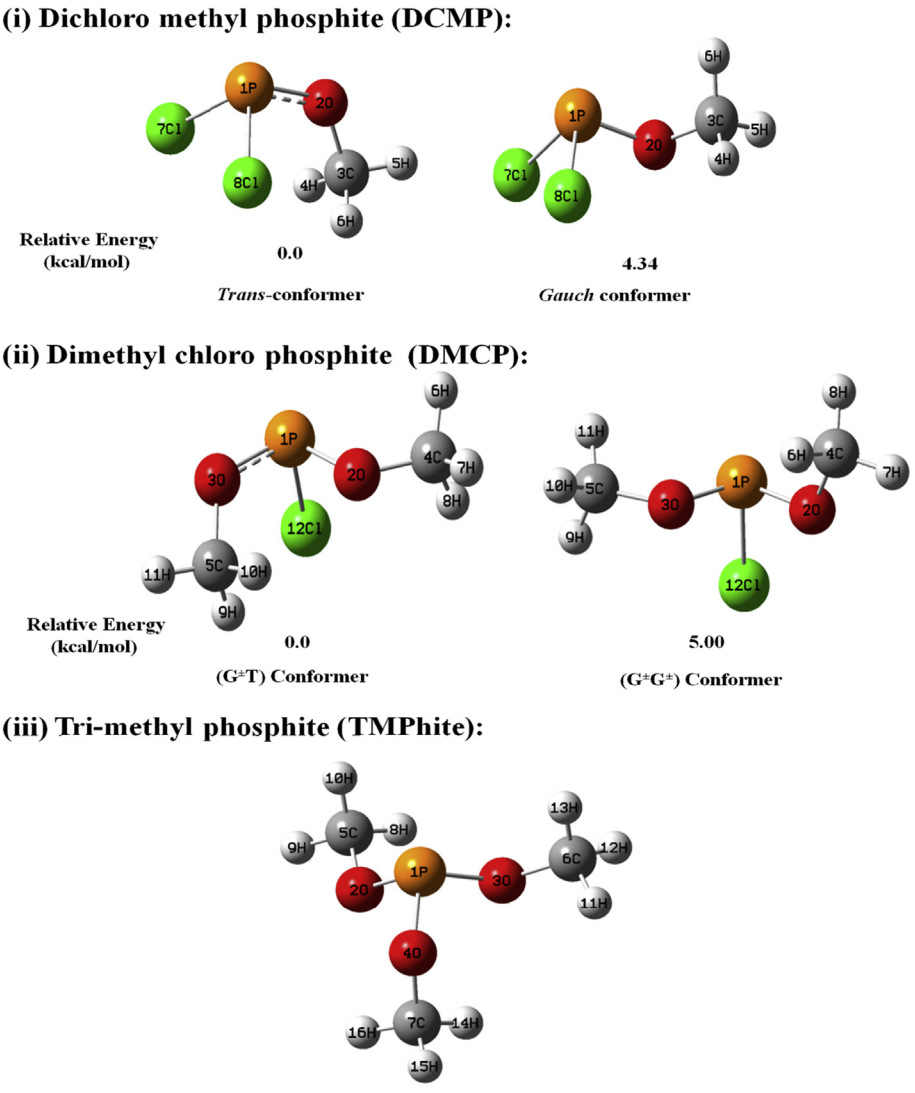

Fig. 4. Computed structures of (i) DCMP, (ii) DMCP and (iii) TMPhite at B3LYP/6-311++G(d,p) level of theory.

Table 1
Comparison between computed and experimental vibrational frequencies of possible products and mode assignment of PCl_3 and CH_3OH reaction.

Vibrational frequencies ν (cm^{-1})											Mode assignment
Experimental (N_2 matrix)	Computed (unscaled) at B3LYP/6-311++G(d,p)					Scaling factor	Computated (scaled) at B3LYP/6-311++G(d,p)				
	DCMP		DMCP		TMPhite		DCMP		DMCP	TMPhite	
	Trans	Gauche	($G^{\pm}T$)	($G^{\pm}G^{\pm}$)			Trans	Gauche	($G^{\pm}T$)	($G^{\pm}G^{\pm}$)	
511.3	483.2 (81)[a]	504.8 (102)	478.5 (55)	486.9 (133)	–	1.0583	511.3	534.2	506.4	515.3	–	$P-Cl$ (ν_1)
469.2, 466.4, 464.5, 462.1	429.7 (195)	442.5 (156)	–	–	–	1.0809	464.4	478.3	–	–	–	$P-Cl$ (ν_3)
753.1	736.1 (83)	742.0 (107)	730.9 (128) 752.1 (80.5)	727.4 (155)	687.7 (186)	1.0231	753.1	759.1	747.8	744.2	703.6	ν_{P-O}
				753.8 (98)	731.0 (154)				769.5	771.2	747.9	
					746.3 (67)						763.5	
1044.4	1053.7 (290)	1036.1 (285)	1042.4 (415)	1033.4 (382)	1030.9 (333)	1047.1 (310) 0.9890	1042.1	1024.7	1030.9	1022.0	1019.6	ν_{C-O}
1042.1			1060.1 (126)	1061.5 (143)	1076.5 (88)				1048.4	1049.8	1035.6	
											1064.2	

[a] Intensities in km/mol given in parentheses.

the excess of CH_3OH present to form DMCP and HCl (Step ii). Interestingly, the IR spectrum (Fig. 1d) showed features similar to that of 1:1 PCl_3:CH_3OH experiment. The only difference is that the intensity of the CH_3Cl features observed are higher for 1:2 PCl_3:CH_3OH experiment (Fig. 3). Two possible explanations could be thought of for this observation: (a) IR frequencies of DMCP are similar to that of DCMP or (b) DMCP produced in Step (ii) is not stable and hence undergoes further reaction (Fig. 2, SR ii). The formation of higher concentration of CH_3Cl (Fig. 3) in 1:2 PCl_3:CH_3OH experiment supports the later explanation. The byproduct, phosphonochloridate formed in the reaction might have low vapor pressures and hence could not be transported to the matrix. Additionally, some contribution of CH_3Cl formation from CH_3OH and HCl reaction, as mentioned in 1:1 PCl_3:CH_3OH experiment, could not be ruled out.

Surprisingly, IR features observed in case of 1:3 PCl_3:CH_3OH experiment shows only CH_3Cl formation whereas the expected trimethyl phosphite (TMPhite) (step iii) was not seen. Here, presence of excess methanol plays a vital role to drive the reaction to completion. As explained earlier, in the first step, PCl_3 reacts to form DCMP and progressed through second (step ii) and third steps (step iii). Finally, the reaction between TMphite and HCl could lead to the formation of CH_3Cl via Arbuzov reaction (Fig. 2). These subsequent reactions could be the possible reason for not observing the infrared features of TMPhite when PCl_3 and CH_3OH were mixed in the 1:3 proportions. Reaction of TMPhite with HCl through Arbuzov pathway to yield CH_3Cl has been reported recently [14]. Other possibility for CH_3Cl formation via the reaction CH_3OH and HCl is also not ruled out. Features of unreacted CH_3OH and HCl are observed in the spectrum (Fig. 1e) for the 1:3 PCl_3:CH_3OH experiment indicating that the contribution of CH_3Cl formed via reaction of CH_3OH and HCl could be comparatively less. This may also be true for 1:2 PCl_3:CH_3OH experiment. The other product, dimethyl hydrogen phosphonate (DMHP) formed during Arbuzov reaction could be hydrolyzed in presence of excess HCl to yield methylhydrogen phosphonate and phosphorus acid, which could have low vapor pressures to be transported to the matrix and thus not observed in the IR spectra.

The amount of HCl obtained (Fig. 3), is more in the 1:2 PCl_3:CH_3OH experiment compared to 1:1 and 1:3 PCl_3:CH_3OH experiments. The source for HCl formation in case of 1:1 PCl_3:CH_3OH experiment is only through the first step. However, in the case of 1:2 and 1:3 PCl_3:CH_3OH experiments, HCl is obtained from the first two and all three steps respectively. In case of 1:3 PCl_3:CH_3OH experiment, entire DCMP is probably converted to TMPhite via DMCP, but the TMPhite formed follows Arbuzov reaction with HCl to form CH_3Cl, thereby consuming some amount of HCl. In the case of 1:2 PCl_3:CH_3OH experiment, presence of higher concentration of DCMP compared to 1:1 PCl_3:CH_3OH experiment reveals that high amount of HCl is also produced as a byproduct during the first step. HCl generated via second step may also add up to the total amount. Additionally, presence of DCMP indicates that the reaction is not complete and less amount of HCl may be utilized during CH_3Cl formation (Fig. 2, SR ii) compared to 1:3 PCl_3:CH_3OH experiment. Therefore, the HCl concentration observed in 1:2 PCl_3:CH_3OH experiment is more compared to other two experiments (Fig. 3).

3.2. Computations

Computations for DCMP, DMCP, and TMPhite at B3LYP/6-311++G(d,p) level of theory were performed, to find out vibrational frequencies and thermochemical properties of all predicted steps of the reaction. Computations revealed two possible conformers, '*gauche*' and '*trans*' for DCMP, two conformers ($G^{\pm}G^{\pm}$) and ($G^{\pm}T$) for DMCP and one conformer for TMPhite as shown in Fig. 4.

In case of DCMP, '*gauche*' conformer is placed at 4.34 kcal/mol with respect to the ground state '*trans*' conformer, indicating a negligible population for the higher energy '*gauche*' conformer. In DMCP, the relative energy between ($G^{\pm}T$) conformer and ($G^{\pm}G^{\pm}$) conformer is 5.00 kcal/mol indicating again that ($G^{\pm}T$) conformer is more stable over ($G^{\pm}G^{\pm}$) conformer. A comparison of computed and experimental vibrational frequencies of DCMP, DMCP and TMPhite is given in Table 1. From the table it is clear that only DCMP has vibrational frequencies for the P–Cl ν_3 and ν_1 modes. The computed spectrum of DCMP and DMCP are compared with the experimental results (Fig. 5). A good agreement of computed frequencies of DCMP with the experimental is seen. On the basis of energetics, *trans*-DCMP conformer could be the most probable conformer produced during PCl_3 and CH_3OH reactions. It is clear from Table 1 that there is a good agreement between the vibrational features obtained in the experiment and the computed frequencies of the '*trans*' conformer of DCMP.

To rationalize the formation of DCMP and CH_3Cl from PCl_3 and CH_3OH experiments of different ratios, free energy calculations for these reactions were performed and shown in Table 2. The change in free energy values were calculated for reactions at B3LYP/6-311++G(d,p) level of theory. The free energy change (ΔG) for the DCMP formation was found to be −9.0 kcal/mol, indicating spontaneity of the reaction. However, ΔG value for CH_3Cl formation from DCMP (Fig. 2, SR i) is 6.0 kcal/mol indicates reaction is non-spontaneous. Thus, as assumed earlier CH_3Cl formation via this reaction is unlikely. This may be due to the presence of two Cl atoms in DCMP which pulls electron cloud and thus lone pair of electrons on phosphorus atom is more delocalized. Thus, simultaneous abstraction of H atom and bond cleavage of HCl, alike Arbuzov reaction, could not be possible. This observation reveals that CH_3Cl formation in 1:1 PCl_3:CH_3OH experiment is most probably via reaction between CH_3OH and HCl. Low intense IR features observed during this experiment agreed with our earlier assumption that contribution of CH_3Cl formation through this reaction is less. Similarly, ΔG calculations for DMCP (step ii) and TMPhite (step iii) formation were found to be −3.0 and −1.0 kcal/mol respectively, indicating spontaneity of the reactions. In 1:2 PCl_3:CH_3OH experiment, DMCP may further undergo reaction with HCl to yield CH_3Cl and ΔG (−2.0 kcal/mol) value also agrees well for CH_3Cl formation through this reaction. Although, one Cl (electron withdrawing) atom in DMCP pulls electron cloud from P atom, this effect could be far less in DMCP relative to DCMP due to the presence of two $-OCH_3$ (electron donating) groups. Thus, lone pair of electron on the P atom may not be delocalized in DMCP and hence abstract H from HCl and this reaction leads to CH_3Cl formation, alike Arbuzov reaction. In short, the formation of CH_3Cl also support our assumption that both, DCMP and DMCP, may be formed during 1:2 PCl_3:CH_3OH experiment but the DMCP may undergo further reaction to yield CH_3Cl and thus IR features of only DCMP and CH_3Cl are observed. In case of 1:3 PCl_3:CH_3OH experiment, CH_3Cl is formed via well known Arbuzov reaction ($\Delta G = -7.0$ kcal/mol).

3.2.1. Comparison with commercial product

To confirm the formation of DCMP in PCl_3–CH_3OH reaction, an experiment has been performed with commercially obtained DCMP in the N_2 Matrix at 12 K. Fig. 5 compares infrared spectrum of commercially procured DCMP (shown in blue color (in the web version)) with infrared spectra obtained during 1:1 and 1:2

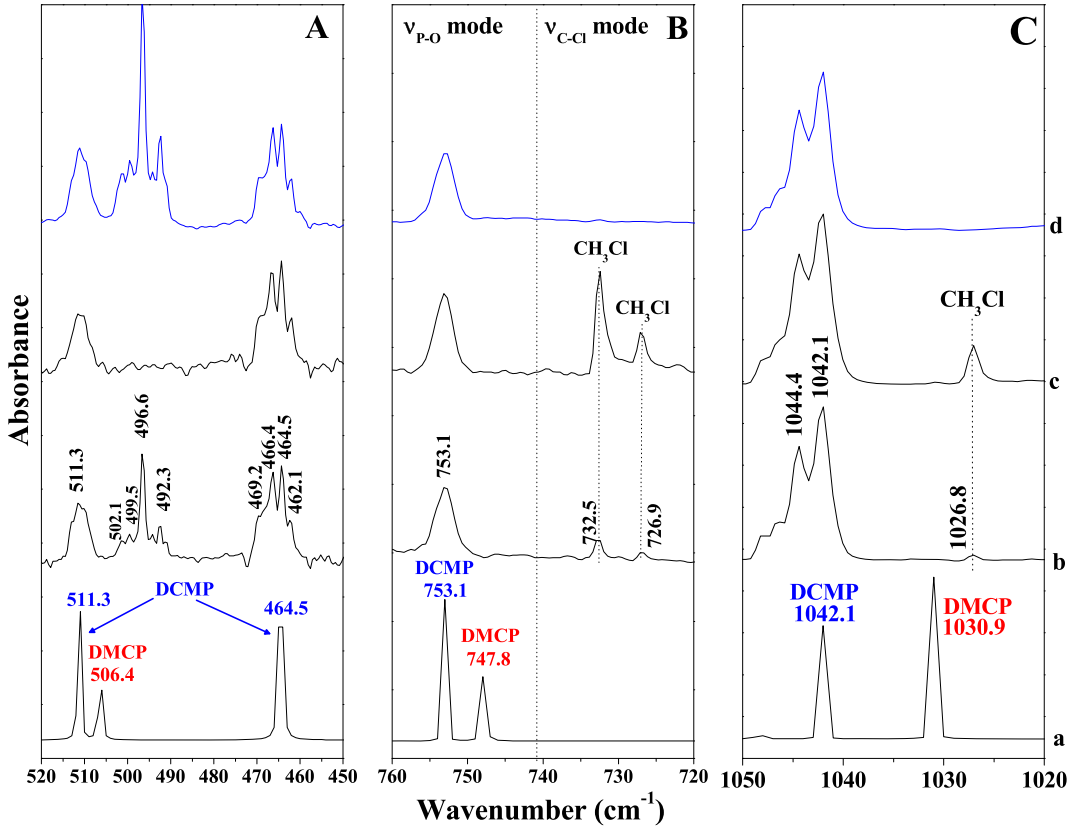

Fig. 5. Comparison of experimental and computed spectra spanning the 520–450 cm^{-1} (Grid A); 760–720 cm^{-1} (Grid B) and 1050–1020 cm^{-1} (Grid C): a) computed spectrum* of DCMP and DMCP; matrix isolation infrared spectra in a N_2 matrix of b) PCl_3:CH_3OH:N_2 (1:1:1000); c) PCl_3:CH_3OH:N_2 (1:2:1000); d) Commercially obtained dichloro methyl phosphite:N_2 (1:1000).*The computed spectra are plotted assuming scaled vibrational frequencies and Lorentzian line profile with the line width of 1 cm^{-1}.

Table 2
Thermodynamic parameters such as, change in internal energies (ΔE), change in enthalpies (ΔH), and change in free energies (ΔG) for two different pathways of PCl_3 and CH_3OH reaction calculated at B3LYP/6-311++G(d,p) level of theory.

Reaction pathways	Thermodynamic Parameters (kcal/mol)		
	ΔE	ΔH	ΔG
Step i)	−10.0	−10.0	−9.0
Step ii)	−5.0	−4.0	−3.0
Step iii)	−2.0	−1.0	−1.0
SR[a] i)	8.0	7.0	6.0
SR ii)	0.5	−1.0	−2.0
SR iii) Arbuzov reaction	−6.0	−7.0	−7.0
AR[b]	−6.0	−6.0	−4.0

[a] SR = side reaction.
[b] AR = alternate reaction.

PCl_3:CH_3OH experiments. The infrared features for commercial DCMP were observed at 469.2, 466.4, 464.5, 462.1, 511.3 cm^{-1} (Fig. 5, grid A), 753.1 cm^{-1} Fig. 5, grid B) and 1044.4 and 1042.1 cm^{-1} ((Fig. 5, grid C). Clearly, a comparison of infrared spectrum of commercial product with the spectra obtained in the PCl_3—CH_3OH premixing experiments (1:1 and 1:2 PCl_3:CH_3OH proportions) allows to attribute the new features observed in the P—Cl, O—C and P—O stretching modes to DCMP.

4. Conclusions

Gas phase reaction between PCl_3 and CH_3OH for various stochiometry was performed and the products were identified using matrix isolation infrared spectroscopy. Infrared spectra obtained for 1:1 and 1:2 PCl_3:CH_3OH ratio experiments revealed the formation of DCMP and HCl as major products along with small concentration of CH_3Cl. In case of 1:3 PCl_3:CH_3OH experiment, only CH_3Cl was observed. These experiments aided us to propose a reaction mechanism for various ratios of PCl_3 and CH_3OH. Mechanism through a nucleophilic substitution has been proposed for PCl_3 and CH_3OH reactions where CH_3OH is the nucleophile.

Acknowledgments

Dr. P. R. J. is thankful to IGCAR, Department of Atomic Energy, India for providing Research Associate fellowship.

References

[1] Y. Ren, Z. Huang, D. Jiang, L. Liu, K. Zeng, B. Liu, X. Wang, Appl. Therm. Eng. 26 (2006) 327.
[2] R. Zhu, X. Wang, H. Miao, Z. Huang, J. Gao, D. Jiang, Energy Fuels 23 (2009) 286.
[3] P.A. Turhanen, R. Niemi, M. Peräkylä, T. Järvinen, J. Vepsäläinen, J. Org. Biomol. Chem. 1 (2003) 3223.
[4] R.L. Letsinger, V.J. Mahadevan, J. Am. Chem. Soc. 87 (1965) 3526.
[5] R.L. Letsinger, K.K. Ogilvie, J. Am. Chem. Soc. 89 (1967) 4801.
[6] R.L. Letsinger, M.H. Caruthers, P.S. Miller, K.K. Ogilvie, J. Am. Chem. Soc. 89 (1967) 7146.
[7] R.L. Letsinger, K.K. Ogilvie, J. Am. Chem. Soc. 91 (1969) 3350.
[8] C.V.S. Brahmmanada Rao, (Ph.D. Thesis), Madras University, 2012.
[9] C.F. Chen, S.F. Lo, S.H. Chen, Diam. Relat. Mater 5 (1996) 766.
[10] H.Y. Xu, S. Xie, Q.Y. Wang, X.L. Yao, Q.S. Wang, C.H. Chen, Electrochim. Acta 52 (2006) 636.
[11] R.V. Hodges, S.A. Sullivan, J.L. Beauchamp, J. Am. Chem. Soc. 102 (1980) 935.
[12] R.C. Lum, J.J. Grabowski, J. Am. Chem. Soc. 114 (1992) 8619.
[13] J.K. Laerdahl, E. Uggerud, Int. J. Mass Spectrom. 214 (2002) 277 (and references therein).
[14] N. Ramanathan, B.P. Kar, K. Sundararajan, K.S. Viswanathan, J. Phys. Chem. A 116 (2012) 12014.
[15] K. Sundararajan, N. Ramanathan, J. Phys. Chem. A 117 (2013) 2347.
[16] M.J. Frisch, G.W. Trucks, H.B. Schlegel, P.M.W. Gill, B.G. Johnson, M.A. Robb, J.R. Cheeseman, T. Keith, G.A. Petersson, J.A. Montgomery, K. Raghavachari, M.A. Al-Laham, V.G. Zakrzewski, J.V. Ortiz, J.B. Foresman, J. Cioslowski, B.B. Stefanov, A. Nanayakkara, M. Challacombe, C.Y. Peng, P.Y. Ayala, W. Chen, M.W. Wong, J.L. Andres, E.S. Replogle, R. Gomperts, R.L. Martin, D.J. Fox, J.S. Binkley, D.J. Defrees, J. Baker, J.P. Stewart, M. Head-Gordon, C. Gonzalez, J.A. Pople, GAUSSIAN 94, Revision D.1, Gaussian Inc., Pittsburgh, PA, 1995.
[17] S. Cradock, A.J. Hinchcliffe, Matrix Isolation: a Technique for the Study of Reactive Inorganic Species, Cambridge University Press, Cambridge, 1975.
[18] G.C. Pimentel, S.W. Charles, Pure Appl. Chem. 7 (1963) 111.
[19] K. Sundararajan, K. Sankaran, K.S. Viswanathan, A.D. Kulkarni, S.R. Gadre, J. Phys. Chem. A 106 (2002) 1504.
[20] N. Ramanathan, K. Sundararajan, B.P. Kar, K.S. Viswanathan, J. Phys. Chem. A 115 (2011) 10059.
[21] N. Ramanathan, K. Sundararajan, J. Mol. Struct. 1034 (2013) 257.
[22] N. Ramanathan, C.V.S. Brahmmananda Rao, K. Sankaran, K. Sundararajan, J. Phys. Chem. A 119 (2015) 4017.
[23] K. Irikura, SYNSPEC, National Institute of Standards and Technology, Gaithesburg, MD, 1995.
[24] M. Hawkins, M.J. Almond, A.J. Downs, J. Phys. Chem. 89 (1985) 3326.
[25] P.R. Joshi, N. Ramanathan, K. Sundararajan, K. Sankaran, J. Phys. Chem. A 119 (2015) 3440.
[26] N. Bakkas, Y. Bouteiller, A. Loutellier, J.P. Perchard, S. Racine, J. Chem. Phys. 99 (1993) 3335.
[27] W.L. Jorgenson, J. Phys. Chem. 90 (1986) 1276.
[28] N. Ramanathan, K. Sankaran, J. Mol. Struct. 1054 (2013) 331.
[29] M. Solimannejad, M. Gharabaghi, S. Scheiner, J. Chem. Phys. 134 (2011) 024312.
[30] S. Scheiner, J. Chem. Phys. 134 (2011) 094315.
[31] S. Scheiner, J. Phys. Chem. A 115 (2011) 11202.
[32] U. Adhikari, S. Scheiner, Chem. Phys. Lett. 536 (2012) 30.
[33] U. Adhikari, S. Scheiner, J. Phys. Chem. A 116 (2012) 3487.
[34] S. Scheiner, U. Adhikari, J. Phys. Chem. A 115 (2011) 11101.
[35] U. Adhikari, S. Scheiner, J. Chem. Phys. 135 (2011) 184306.
[36] U. Adhikari, S. Scheiner, Chem. Phys. Lett. 532 (2012) 31.
[37] S. Scheiner, Acc. Chem. Res. 46 (2013) 280.
[38] S. Scheiner, Int. J. Quant. Chem. 113 (2013) 1609.
[39] I. Alkorta, G. Sanchez-sanz, J. Elguera, J.E. Del Bene, J. Phys. Chem. A 117 (2013) 183.
[40] J.E. Del Bene, I. Alkorta, G. Sanchez-sanz, J. Elguera, Chem. Phys. Lett. 512 (2011) 184.
[41] J.E. Del Bene, I. Alkorta, G. Sanchez-sanz, J. Elguera, J. Phys. Chem. A 115 (2011) 13724.
[42] J.E. Del Bene, I. Alkorta, G. Sanchez-sanz, J. Elguera, J. Phys. Chem. A 116 (2012) 3056.
[43] J.E. Del Bene, I. Alkorta, J. Elguera, J. Phys. Chem. A 118 (2014) 2360.